

Effect of Water on the Mechanical Properties of Wood Cell Walls – Results of a Nanoindentation Study

Leopold Wagner,^{a,*} Clémence Bos,^{a,b} Thomas K. Bader,^a and Karin de Borst^c

The paper presents a nanoindentation study on five different wood species in which the elastic and creep properties of the S2 cell wall layer and the middle lamella were determined. Measurements were carried out at relative humidities (RH) ranging from 10 to 80% as well as underwater. Indentation moduli were found to decrease by about a third in the S2 layer and by about half in the middle lamella between RH of 10 and 80%. Hardness dropped by 50 to 60% in this humidity range in both the S2 layer and the middle lamella. Creep parameters were almost constant up to a relative humidity of 40%, but they increased considerably at higher RH. The most pronounced change of reduced moduli and creep properties occurred between 60 and 80% RH, which is consistent with the expected softening of hemicellulose and amorphous parts of cellulose in this humidity region. Immersion into water resulted in a further decrease of the reduced moduli to about 20 to 30% of their values at 10% RH and to only about 10 to 20% for the hardness. This can be explained by additional softening of the less ordered regions of cellulose.

Keywords: Nanoindentation; Cell wall; Moisture effects; Creep; Hardwood; Softwood

*Contact information: a: Institute for Mechanics of Materials and Structures, Vienna University of Technology, Karlsplatz 13/202, 1040 Vienna, Austria; b: Institute for Applied Materials, Karlsruhe Institute of Technology, Hermann-von-Helmholtz-Platz 1, 76344 Eggenstein-Leopoldshafen, Germany; c: School of Engineering, University of Glasgow, Glasgow G12 8LT, Scotland, United Kingdom; * Corresponding author: leopold.wagner@tuwien.ac.at*

INTRODUCTION

Adsorbed water significantly reduces the mechanical strength of wood. Individual water molecules are able to diffuse into the wood cell wall ultrastructure and to act as a softening agent. Using nanoindentation, this effect can be studied at the cell wall scale. This eliminates the influences of the cellular structure and the overall mass density of wood, which complicate comparisons between different samples of different wood tissues. Moreover, testing at smaller length scales allows for the probing of different cell wall layers individually. Their different compositions and structures should deliver insight into the effects of water on the material and its mechanical behavior.

Nanoindentation was applied to samples of five different wood species, which had undergone extensive microstructural characterization, at four different relative humidities (RH) between 10 and 80% as well as underwater. Both the S2 cell wall layer, which is by far the thickest and stiffest layer, and the middle lamella, which connects neighboring wood cells, were tested. These two layers are crucial for load transfer in wood. The S2 layer withstands axial loads whereas the middle lamella controls the behavior of the wood under shear and in bending. In addition to the reduced modulus, the hardness and creep parameters, in terms of increased deformation under constant loading, were determined.

Measurements of macroscopic samples typically show a drop in the elastic moduli of 10 to 20% in longitudinal direction and 5 to 25% in the radial and tangential directions when the moisture content (and thus, the relative humidity) increases from 12 to 20% (Gerhards 1982). Stiffness reductions of similar magnitude were observed in single wood fibers (Kersavage 1973; Eder 2007). Ehrnrooth and Kolseth (1984) obtained ratios between 2.47 and 4.75, with a mean of 3.07, for the elastic modulus of a spruce fiber at 50% RH and water-soaked condition, respectively. The same authors reported an increase of displacement up to about 10% over a period of 10 s depending on the applied load. Olsson *et al.* (2007) observed creep strain rates of 0.041 and 0.044%/s in spruce fibers at stresses of 280 and 440 MPa, respectively, at 80% RH.

Nanoindentation has been applied before to study the elastic behavior of wood cell walls at different relative humidities (Yu *et al.* 2011; Bertinetti *et al.* 2014; Li *et al.* 2014). Yu *et al.* (2011) reported a linear decrease in the reduced modulus and indentation hardness of Masson pine by 17 and 33% from 20 to 70% RH, respectively. The corresponding creep rate at constant load was about 1.5 to 1.8 nm/s at between 20 and 40% RH which increased to 2.2 nm/s at 70% RH. Li *et al.* (2014) reported no significant changes in the creep rate of Masson pine cell walls in the range of 20 to 40% RH, whereas increasing microfibril angle (MFA) led to higher creep rates. They also reported the reduced modulus and hardness to decrease by 6.5 to 12.3% and 11.9 to 24.4%, respectively, with increased RH from 20 to 60%, depending on the MFA. Recently, Bertinetti *et al.* (2014) published moisture-dependent experimental data for the S2 layer in spruce wood between 6 and 79% RH, showing that the reduced modulus and hardness decreased by about 40 and 66% across this humidity range, respectively.

The current study goes beyond existing investigations by systematically examining the stiffness, hardness, and creep properties of the S2 layer and the ML. Moreover, the testing of five different wood species, both softwood and hardwood, with known microstructural characteristics allowed conclusions about the relationship between indentation behavior and the sample microstructure to be drawn. These investigations contribute to an improved understanding of moisture effects on mechanical properties of wood as well as of wood based products.

EXPERIMENTAL

Samples

Investigations were carried out on wood samples of three softwood species, Norway spruce (*Picea abies* [L.] Karst.), common yew (*Taxus baccata* L.), and Scots pine (*Pinus sylvestris* L.), as well as two hardwood species, European beech (*Fagus sylvatica* L.) and European oak (*Quercus robur* L.). The sample material was subjected to microstructural and compositional characterization (Bader *et al.* 2012; de Borst *et al.* 2012; Wagner *et al.* 2013) which are summarized in Table 1. Small wood specimens (approximately 1.5 x 2 x 1 mm³ in the longitudinal, radial, and tangential directions) were cut from the latewood (LW) region of annual rings investigated in the mentioned characterization campaign. Following the protocol proposed by Wagner *et al.* (2014) for the sample preparation, the specimens were embedded in an epoxy resin (AGAR Low Viscosity Resin Kit, Agar Scientific, Essex, UK) to stabilize the wood cell walls. The cross sectional surface of the embedded samples was cut smooth using a microtome equipped with a diamond knife. The specimens were stored in ambient conditions of 20±2 °C and

30 to 40% relative humidity (RH) prior to embedding and were heated to 60 °C for 24 h during resin curing (Wagner *et al.* 2014), partially drying the samples. After curing, the samples were conditioned under the same ambient conditions again.

Table 1. Microfibril angle (MFA) and Composition in Terms of Mass Fractions of Cellulose (w_{CEL}), Hemicelluloses (w_{HC}), Lignin (w_{LIG}), and Extractives (w_{EXT}) of the Investigated Wood Samples

Species	MFA (°)	w_{CEL} (%)	w_{HC} (%)	w_{LIG} (%)	w_{EXT} (%)	Ref.
Scots pine	12.7	46.9	27.1	23.5	2.5	a
Norway spruce	12.5	49.1	24.4	23.7	2.8	b
Common yew	27.0	44.7	20.8	23.9	10.6	b
European oak	3.0	40.8	32.2	21.0	6.0	c
European beech	7.0	49.1	25.0	23.2	2.7	c

a: Wagner *et al.* (2013), b: Bader *et al.* (2012), c: de Borst *et al.* (2012)

Nanoindentation

The nanoindentation tests were carried out using a Triboindenter® (Hysitron Inc., Minneapolis, MN, USA) equipped with a three-sided, pyramid-shaped tip (Berkovich type) in load-controlled mode. The measurement chamber of the Triboindenter® was climatized to 22 ± 1 °C and stepwise to 10, 40, 60, and 80% RH using a RH-200 Relative Humidity Generator (L&C Science and Technology, Hialeah, FL, USA). The limits of 10% and 80% RH arise from technical limitations of the equipment employed. The samples were conditioned inside the measurement chamber overnight prior to the tests (Yu *et al.* 2011, Li *et al.* 2014). For the tests underwater (*i.e.*, under fully saturated conditions), the sample was put in a small container. This container was clamped to the magnetic table of the Triboindenter® by means of small steel discs onto which the specimens were mounted during sample preparation. To limit the variability of the results, all indentations were performed within an area of approximately $200 \times 200 \mu\text{m}^2$ within the LW region of each sample. The position of the indentations on the respective cell wall was chosen from scanning probe microscopy (SPM) images recorded with the built-in SPM in the Triboindenter®. For the underwater tests, the indenter tip was removed from the surface after SPM imaging, and the container was then filled with water until the sample was covered by approximately 2 mm of water. Indentations were performed 30 min after immersion (Yu *et al.* 2011). Indentations were placed in the S2 layer of the LW cells, as well as in the middle lamella (ML) in the cell corners between those LW cells. The applied two-level load function consisted of loading to half of the later applied maximum load F_{MAX} , holding that load level for 15 s, partially unloading to one quarter of F_{MAX} , reloading to F_{MAX} , holding that load level for another 15 s, and then completely unloading. This rather complicated load function was chosen to obtain information about the influence of the loading level on the observed creep behavior. F_{MAX} was set to 200 μN for the S2 layer and to 130 μN for the ML. These loads had to be reduced to 150 (S2) and 90 μN (ML) for the tests at 80% RH and under water to fulfil the required distance of the indentation to the nearest interface to avoid possible edge effects (Jakes *et al.* 2009). The resulting load-penetration depth curves were analyzed following the approach of Oliver and Pharr (1992), relating the initial slope of the unloading segments of the curves (initial unloading stiffness S) to the so-called reduced modulus E_r by,

$$E_r = \frac{\sqrt{\pi}S}{2\sqrt{A_C}} \quad (1)$$

where A_C is the contact area, and dividing F_{MAX} by A_C yields the indentation hardness H . In addition, the indentation creep C was defined as follows,

$$C = \frac{h_1 - h_0}{h_0} * 100\% \quad (2)$$

where h_0 and h_1 are the indentation depths at the start and end of the holding phases, respectively (CSM Instruments 2002). The indentation depths at half and full load lie within the range in which no effects of the indentation depth on E_r and H , beyond experimental scatter, are to be expected (Tze *et al.* 2007; Wagner *et al.* 2013). Thus, E_r and H were evaluated at half and full load together. Less is known about the potential influences of indentation depth on the creep behavior, so C was evaluated separately for the first ($C1$) and second holding phase ($C2$). A statistical analysis (ANOVA) was performed to show whether results at higher RH are significantly different ($p=0.01$) from measurement results at 10% RH.

RESULTS AND DISCUSSION

The results of the nanoindentation tests are shown in Figs. 1 to 4 and in Tables 1 and 2 in the Appendix in terms of the sample-specific reduced moduli, hardness values, and creep parameters of ML and S2 as functions of the relative humidity. Inter-species trends at a certain relative humidity can be identified by the same color. The observed trends were similar for the ML and the S2 layers across all species. They were well in line with previous measurements on fibers and cell walls reported before.

A comparison of the results of this study with previously obtained stiffness and hardness data for the same species (Yu *et al.* 2011; Bertinetti *et al.* 2014; Li *et al.* 2014) is shown in Fig. 5. From the current study, only results for softwood samples with comparable MFA (*i.e.*, spruce and pine) are included. The indentation property trends over varying RH observed in different studies were consistent. Also, the absolute values of the reduced moduli and hardness of the S2 layer were close to each other. This is remarkable, since different types of sample preparation methods were used in the previous studies. Yu *et al.* (2011) and Li *et al.* (2014) tested Spurr resin-embedded samples, as in this study, while Bertinetti *et al.* (2014) used cryo-ultramicrotome-cutting of ice-embedded samples to avoid resin embedding. The comparability of the results indicates that the sample preparation method does not significantly affect the measurement results even when the samples are tested under varying moisture conditions. For a constant relative humidity of approximately 60%, Wagner *et al.* (2014) recently showed that the testing of embedded wood cells does not give significantly different properties compared to those of non-embedded cell walls. This is in line with previous investigations suggesting that there is only limited access of the resin to the cell wall ultrastructure (Kamke and Lee 2007). Conclusive evidence on the effect of the embedding resin is still scarce, mainly due to local variability in the cell wall ultrastructure and, consequently, in the indentation properties.

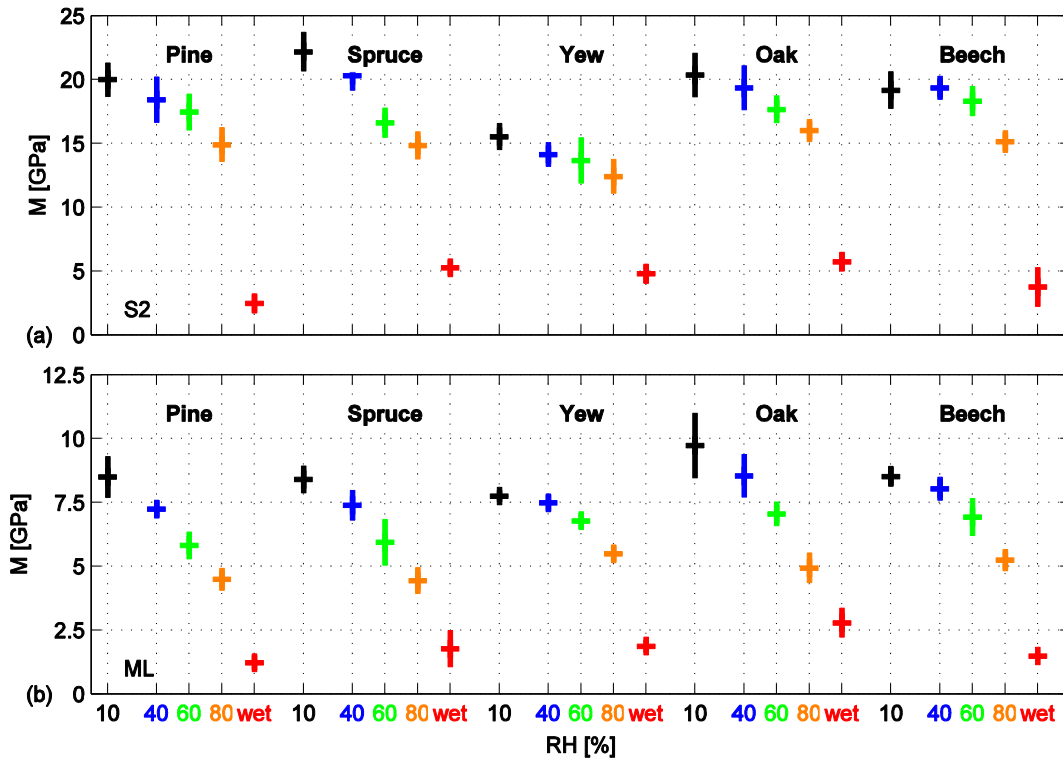


Fig. 1. Reduced moduli E_r in (a) S2 layer and (b) middle lamella (ML) at different relative humidities (RH)

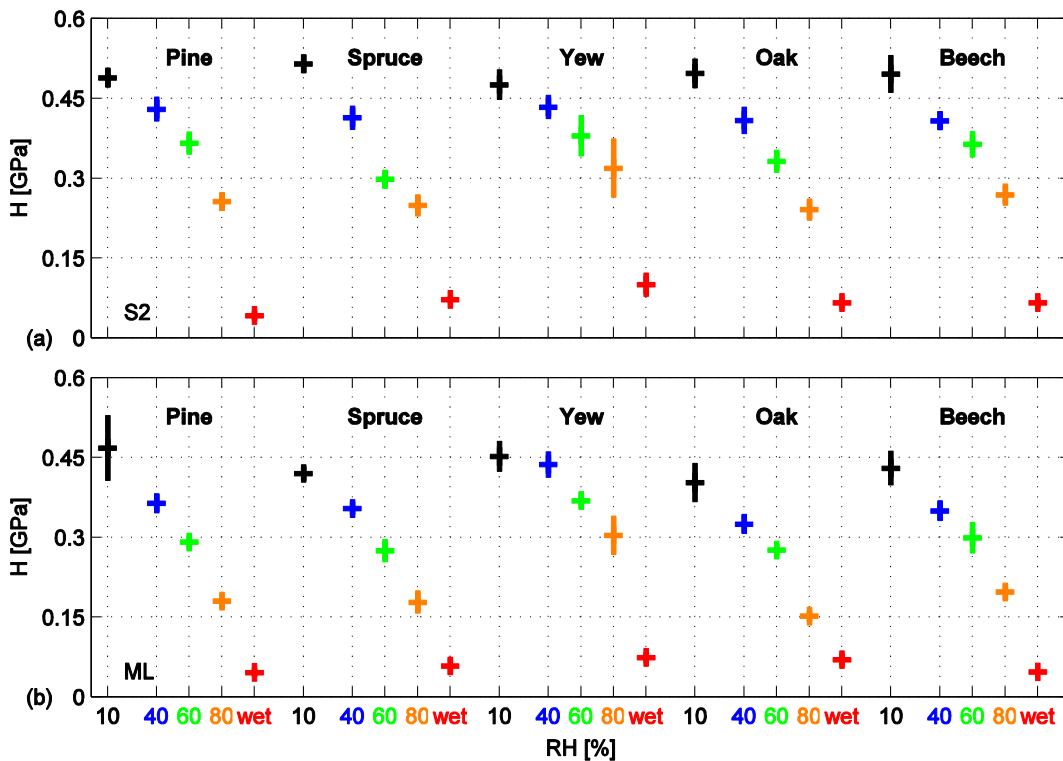


Fig. 2. Hardness H in (a) S2 layer and (b) middle lamella (ML) at different relative humidities (RH)

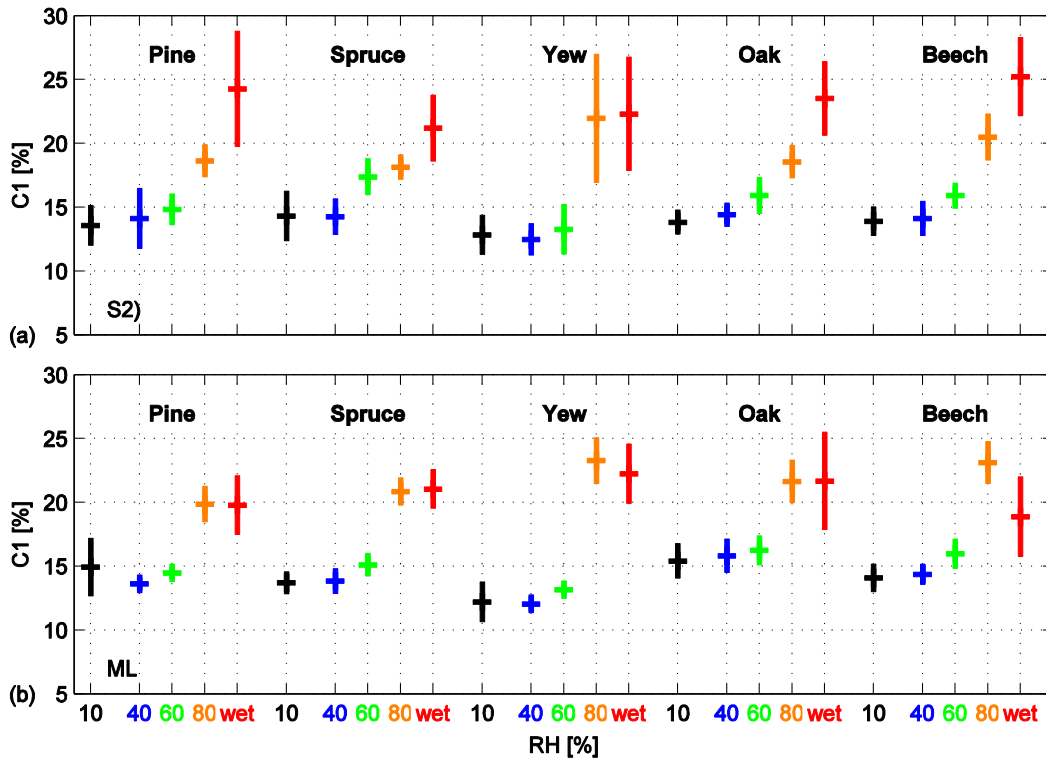


Fig. 3. First creep parameter $C1$ in (a) S2 layer and (b) middle lamella (ML) at different relative humidities (RH)

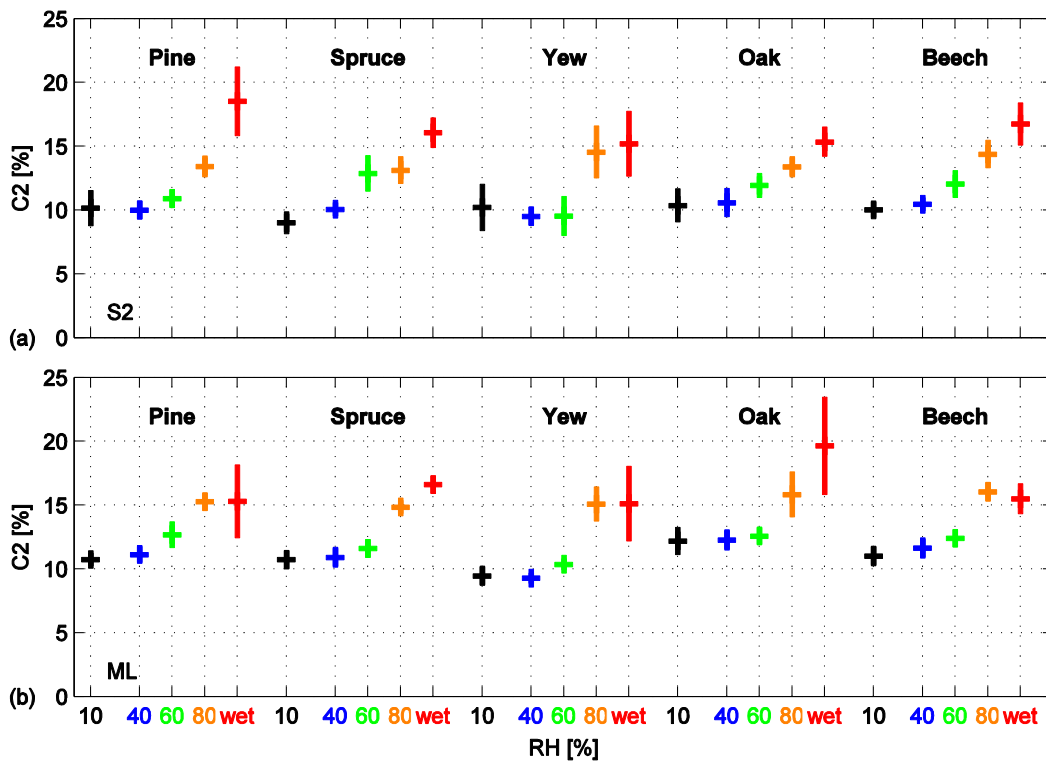


Fig. 4. Second creep parameter $C2$ in (a) S2 layer and (b) middle lamella (ML) at different relative humidities (RH)

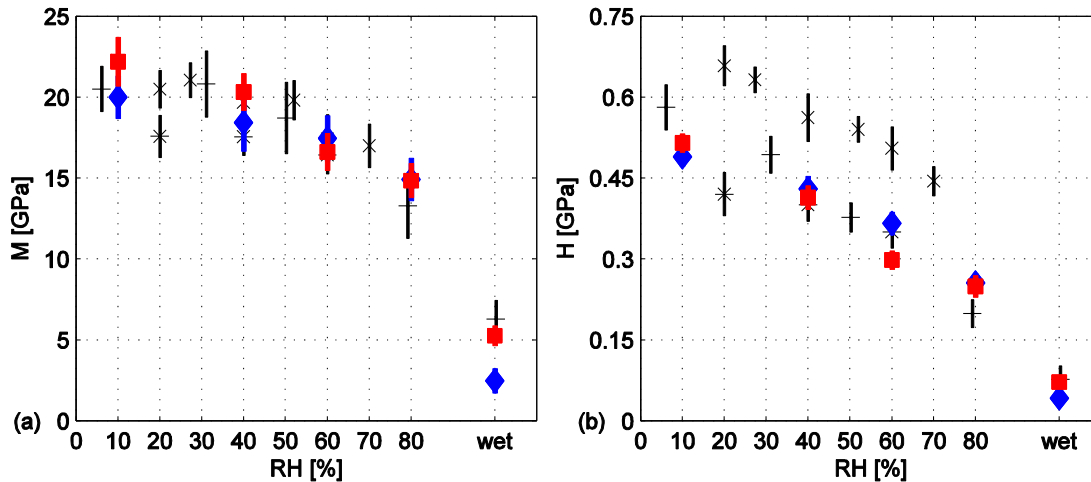


Fig. 5. (a) Reduced moduli E_r and (b) hardness H of softwood vs. RH determined in this study (red: spruce, blue: pine) with respect to previous results from literature; x: Yu *et al.* (2011) (pine), *: Li *et al.* (2014) (pine) +: Bertinetti *et al.* (2014) (spruce)

The effect of the resin is less crucial for hardwood species, where most of the lumens of hardwood fibers were not accessible to the resin. To further elucidate the influence of relative humidity on the indentation results, and to allow comparisons between the samples, relative courses of the indentation results were plotted (Figs. 6 to 7), with the values at 10% RH serving as references. In the following discussions it must be kept in mind that the actual moisture contents at a given relative humidity may vary between the S2 layer and the middle lamella and across species.

Reduced Moduli

In the middle lamella (ML), the modulus at 80% RH was around half of its value at 10% RH, which was rather consistent across species. In the S2 layer, the reduced modulus dropped to around 0.7 and exhibited higher variability between species than the ML. This variability could stem from the different microfibril angles (MFA) of the samples: higher ratios were observed for the hardwood samples with lower MFAs than for the softwood samples with higher MFAs (Table 1). At higher MFA, the cell wall behavior is more strongly influenced by the amorphous matrix in between the cellulose fibers (Kojima and Yamamoto 2005), which are more strongly affected by moisture. Higher reduced moduli at lower MFA were also measured by Li *et al.* (2014).

For all species and for both the S2 and the ML, only very small changes were observed at relative humidities below 40%, which nevertheless have been shown to be statistically significant, with only few exceptions (Appendix Tables 1 and 2). As humidity increased further, the ML curves consistently bent downwards, indicating a pronounced drop in the reduced moduli. The trends were not as consistent for the S2 layer. For pine, yew, and oak, a significant decline occurred only above a relative humidity of 60%. For spruce and oak, the steepest part of the curves occurred between 40 and 60% RH and the curves leveled out above 60% RH. This resulted in a somewhat S-shaped course of the curves.

The strongest decrease in the reduced moduli happened in humidity regions where the amorphous polysaccharides (hemicellulose and amorphous cellulose) are expected to soften (Cousins 1978; Kelley *et al.* 1987; Stelte *et al.* 2011). This softening arises from

water molecules diffusing into the cell wall ultrastructure breaking more and more hydrogen bonds between hemicellulose and amorphous cellulose molecules (Salmén 1982). Moreover, the water molecules reduce the glass transition temperatures of the wood polymers, which results in an additional decrease of the cell wall stiffness (Salmén 1982). Thus, the crystalline sections in the wood cell wall exerted an immobilizing effect on the amorphous parts, shifting the glass transition to higher humidities.

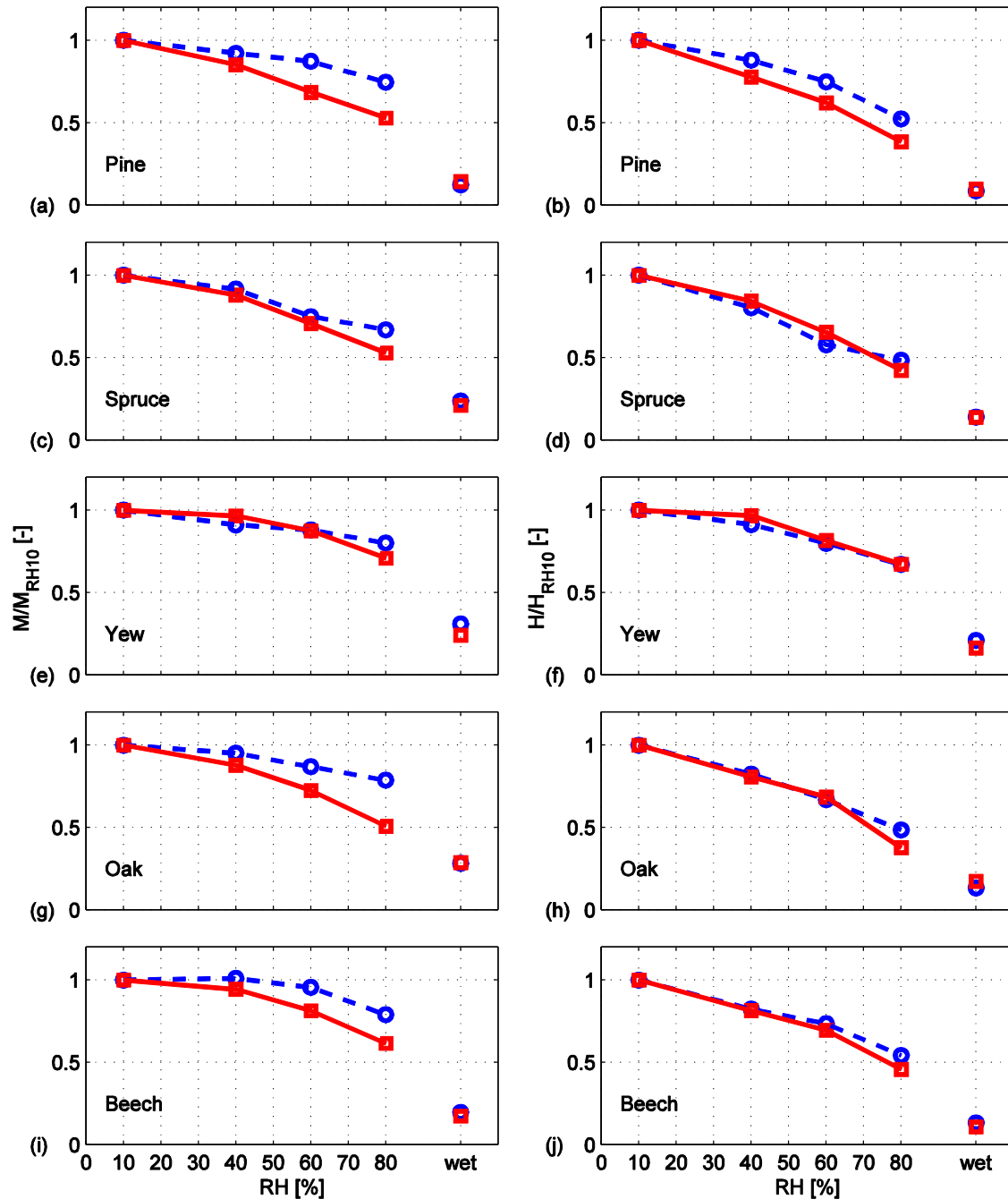


Fig. 6. Relative course of reduced modulus E_r (left) and hardness H (right) over relative humidity (RH) for S2 layer (blue) and ML (red); spruce (a,b), pine (c,d), yew (e,f), oak (g,h), and beech (i,j)

The influence of the crystalline sections decreases with increasing distance from the crystallites, resulting in a very gradual transition spanning a large humidity range (Salmén 1982; Struik 1987), as observed in the indentation results. A real transition-type behavior with an S-shaped curve was only observed for the S2 layers of spruce and oak (Fig. 6).

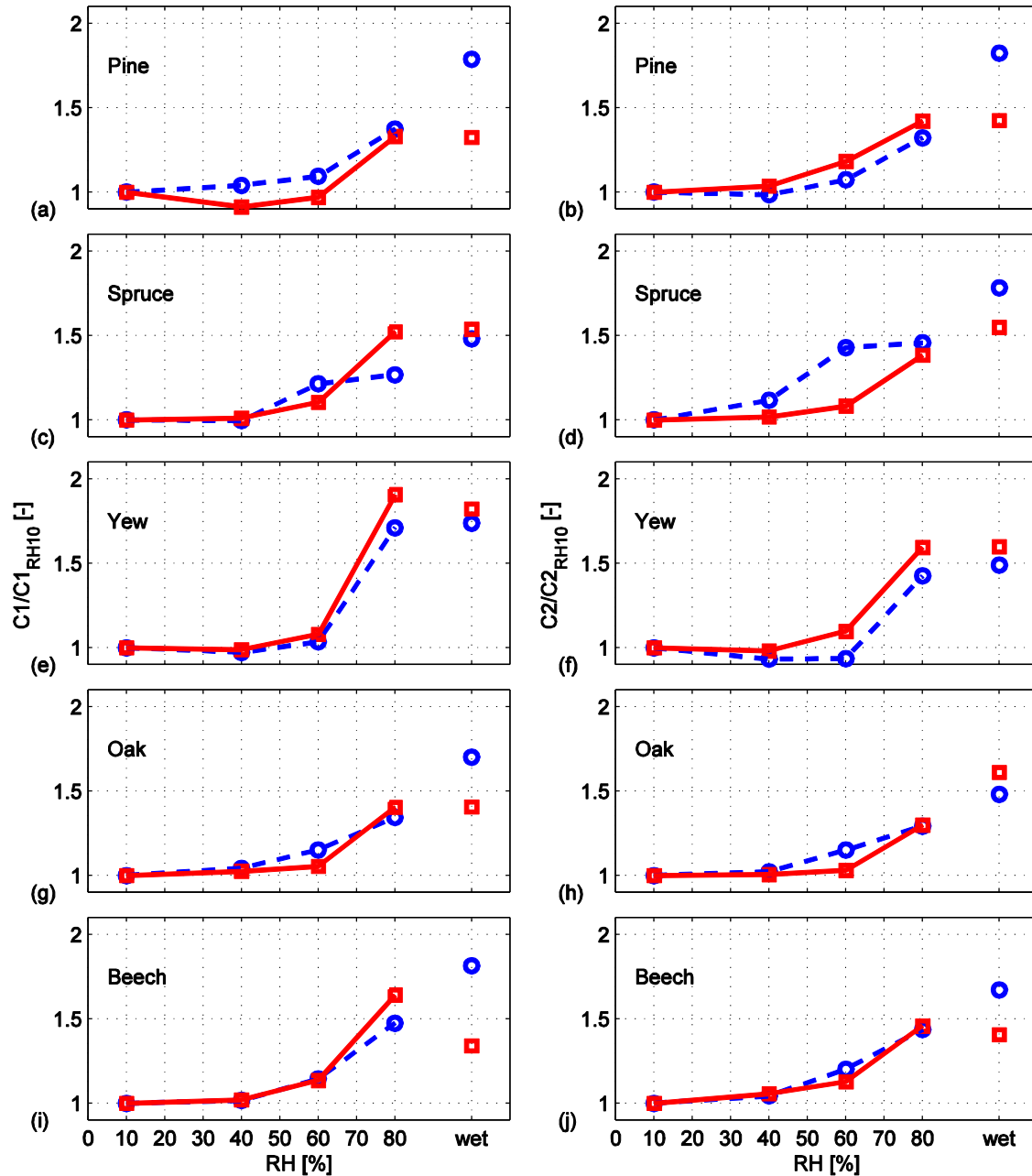


Fig. 7. Relative course of first creep parameter $C1$ (left) and second creep parameter $C2$ (right) over relative humidity (RH) for S2 layer (blue) and ML (red); spruce (a, b), pine (c, d), yew (e, f), oak (g, h), and beech (i, j)

For the other species and the ML, only a downward turn was found. The backward bend and a levelling of the curves at a lower stiffness level may only occur at relative humidities above 80%, which were not examined in this study. When immersed in water, the reduced moduli of the ML and the S2 layer leveled out at similar values relative to the initial moduli, typically in the range of 20 to 30% of their values at 10% RH. The ratios tended to be slightly lower for the ML. Upon immersion in water, the less ordered regions of cellulose also were penetrated by water molecules, *i.e.* softened, resulting in a larger drop of the modulus and thus, another step change compared to the level resulting from the glass transition of the hemicelluloses alone (Salmén 1982).

Hardness

While the reduced moduli are strongly related to the amount and orientation of cellulose, indentation hardness is not directly affected by the MFA (Tze *et al.* 2007) but more closely related to cell wall matrix properties (Gindl *et al.* 2004; Eder *et al.* 2013). Consequently, the variability in hardness across wood species was considerably smaller than the variability in the reduced modulus (Fig. 2). Also, the difference in hardness between S2 and ML was small, with a slightly harder S2 layer. This can be explained by the different chemical composition of these two layers.

The small differences in the absolute hardness values between species and layers naturally resulted in very similar relative courses of the hardness over relative humidity for all wood species and for both S2 and ML. The decreasing trend of H from 10% to 40% was statistically significant, with only few exceptions (Appendix Tables 1 and 2). At 80% RH, hardness values dropped to about 40 to 50% of their values at 10% RH (Fig. 6). The hardness of the S2 layer is more sensitive to humidity changes than the reduced modulus. This confirms a close relationship between the hardness and the cell wall matrix properties, resulting in a strong effect of the softening of the hemicelluloses. Yew exhibited a slightly different behavior with less sensitive hardness. This may be a consequence of the lower moisture content of yew at the same RH as compared to those of the other species due to the exceptional ultrastructure of yew (Table 1). Upon immersion in water, the hardness decreased more strongly than the reduced modulus, where values are typically in the range of 10 to 20% of the values at 10% RH.

Creep Parameters

The influence of moisture on the creep parameters was more pronounced than for the reduced moduli. The second creep parameter C_2 (Fig. 7), related to the second holding phase at maximum load, was consistently about 25 to 30% lower than the first parameter C_1 (Fig. 7), related to the first holding phase at half of the maximum load. An explanation for this trend, although counterintuitive, is that the higher load causes plastic deformations and potential micro-damage in a larger area and may reduce creep in these zones. The creep parameters exhibited similar trends in all samples, though the variability was higher than for the reduced moduli and hardnesses.

The lower creep values in the ML of beech at 80% RH than in the wet state may have been caused by local inhomogeneity of the sample at the positions where C_1 and C_2 were measured. Indeed, while C_1 and C_2 were measured at exactly the same point without moving the indenter tip in between measurements, the tests at different RHs could only be realized in close vicinity to each other.

The creep parameters exhibited similar patterns as the reduced moduli and hardness values, though with a sharper turn of the curves at high humidities. Their respective

changes, with respect to the values at 10% RH, only became significant at higher RH, *i.e.* at 60% and 80% RH (Appendix Tables 1 and 2). Ratios between creep parameters below 40% RH and at 80% RH ranged between 1.3 and 2. The distinct upward bend of all creep curves suggests a significant increase in the creep in the rubbery state after going through the glass transition. Consistent with the results for the reduced moduli and the hardness, a real transition was only observed for the S2-layer of spruce, which exhibited an S-shaped course of the creep parameters over relative humidity. For all other samples, only the upward trend was resolved in the tests, suggesting again that the levelling of the curves only happened at higher relative humidities than those investigated in this test series. The increase of creep at high relative humidity was most pronounced for the yew sample. The high MFA of yew resulted in a more immediate effect of the behavior of the amorphous matrix on the indentation behavior and, thus, on its softening upon moistening, which is in line with findings of the influence of the MFA on the creep behavior of wood at the macroscopic scale (Kojima and Yamamoto 2005).

The observations of strongly enhanced creep at high humidities seemed to be in contrast with the findings of Li *et al.* (2014), who reported no significant influence of the MC on the creep behavior. However, the highest relative humidity investigated by these authors was 60% RH. In the current test series, the upward bend of the creep parameters in the pine sample only happened between relative humidities of 60 and 80%.

The creep parameters of the S2 layer showed only a rather small further increase when the samples were immersed in water. In the middle lamella, they even remained relatively constant. Unlike the reduced moduli, the softening of less ordered parts of the cellulose, in addition to the hemicelluloses, did not seem to cause significant additional creep.

CONCLUSIONS

1. Nanoindentation was applied to investigate the influences of moisture on the elastic and creep properties of wood cell walls. The S2 layer and the middle lamella of five different wood species (spruce, pine, yew, beech, and oak) were tested at relative humidities between 10 and 80%, as well as with the specimens immersed in water.
2. Indentation moduli were found to decrease significantly with increasing humidity. They dropped by about a third in the S2 layer and by about a half in the middle lamella between relative humidities of 10 and 80%.
3. In general, variability was higher in the S2 layer, which likely is a consequence of the varying microfibril angle in this layer.
4. Consistent with the stronger effect of moisture on the hemicellulose-lignin matrix compared to that on cellulose fibers, the effect of moisture was more pronounced in the middle lamella and increased in the S2 layer with rising microfibril angle.
5. Unlike the reduced modulus, hardness was less sensitive to the microfibril angle and more directly related to the matrix properties. Accordingly, only small variations were found between species and between the S2 layer and the ML.
6. Softening of the hemicelluloses can explain the pronounced decrease in stiffness and hardness and the increase in creep starting at relative humidities of 60 to 80%. The results for the S2 layer of spruce clearly show a transition between a regime of high

stiffness and hardness at low humidities and a regime of low stiffness and hardness at high humidities. For the other samples, the backward bend was not observed because testing did not include relative humidities higher than 80%.

7. Immersion into water resulted in a further drop of the reduced modulus to about 20 to 30% of its value at 10% relative humidity. This was likely a consequence of the additional softening of less ordered regions of the cellulose fibers.
8. The creep data exhibited even sharper turns at relative humidities of 60 to 80%, in combination with only small effects of humidity at lower humidity levels. This further suggests that hemicellulose softening was the reason for the observed, pronounced changes in the mechanical behavior.
9. As for creep, softening of hemicellulose seemed to be necessary to activate this process. Immersion into water only affected the creep behavior of the S2 layer, but not of the middle lamella. A further increase in creep by about 30% again indicates that immersion caused additional softening in the cellulosic regions of the S2 layer.

ACKNOWLEDGMENTS

The authors acknowledge the Vienna University of Technology Library for financial support through its Open Access Funding Program.

REFERENCES CITED

- Bader, T. K., Hofstetter, K., Eberhardsteiner, J., and Keunecke D. (2012). "Microstructure-stiffness relationships of common yew and Norway spruce," *Strain* 48(4), 306-316. DOI: 10.1111/j.1475-1305.2011.00824.x
- Bertinetti, L., Hangen, U. D., Eder, M., Leibner, P., Fratzl, P., and Zlotnikov, I. (2014). "Characterizing moisture-dependent mechanical properties of organic materials: humidity-controlled static and dynamic nanoindentation of wood cell walls," *Philos. Mag.* (published online). DOI: 10.1080/14786435.2014.920544
- de Borst, K., Bader, T. K., and Wikete, C. (2012). "Microstructure-stiffness relations of ten European and tropical hardwood species," *J. Struct. Biol.* 177, 532-542. DOI: 10.1016/j.jsb.2011.10.010
- Cousins, W. J. (1978). "Young's modulus of hemicellulose as related to moisture content," *Wood Sci. Technol.* 12(3), 161-167.
- CSM Instruments (2002). "Overview of mechanical testing standards," *Applications Bulletin* No. 18.
- Eder, M. (2007). "Structure, properties and function of single wood fibres of Norway spruce (*Picea abies* [L.] Karst.)," Ph.D. thesis, Universität für Bodenkultur (BOKU), Wien.
- Eder, M., Arnould, O., Dunlop, J.W.C., Hornatowska, J., and Salmén, L. (2013). "Experimental micromechanical characterization of wood cell walls," *Wood Sci. Technol.* 47(1), 163-182. DOI: 10.1007/s00226-012-0515-6
- Ehrnrooth, E. M. L., and Kolseth, P. (1984). "Tensile testing of single wood pulp fibers in air and water," *Wood Fiber Sci.* 16(4), 549-566.

- Gerhards, C. C. (1982). "Effect of moisture content and temperature on the mechanical properties of wood: An analysis of immediate effects," *Wood Fiber* 14(1), 4-36.
- Gindl, W., Gupta, H. S., Schöberl, T., Lichtenegger, H. C., and Fratzl, P. (2004). "Mechanical properties of spruce wood cell walls by nanoindentation," *Appl. Phys. A* 79(8), 2069-2073. DOI: 10.1007/s00339-004-2864-y
- Jakes, J. E., Frihard, C. R., Beecher, J. F., Moon, R. J., Resto, P. J., Melgarejo, Z. H., Suarez, O. M., Baumgart, H., Elmustafa, A. A., and Stone, D. S. (2009). "Nanoindentation near the edge," *J. Mater. Res.* 24(3), 1016-1031. DOI: 10.1557/JMR.2009.0076
- Kamke, F. A., and Lee, J. N. (2007). "Adhesive penetration in wood – A review," *Wood Fiber Sci.* 39(2), 205-220.
- Kelley, S. S., Timothy, G. R., and Glasser, W. G. (1987). "Relaxation behaviour of the amorphous components of wood," *J. Mater. Sci.* 22(2), 617-624.
- Kersavage, P. (1973). "Moisture content effect on tensile properties of individual Douglas-fir latewood tracheids," *Wood Fiber* 5(2), 105-117.
- Kojima, Y., and Yamamoto, H. (2005). "Effect of moisture content on the longitudinal tensile creep behavior of wood," *J. Wood Sci.* 51(5), 462-467. DOI: 10.1007/s10086-004-0676-5
- Li, W., Wang, H., Wang, H., and Yu, Y. (2014). "Moisture dependence of indentation deformation and mechanical properties of Masson pine (*Pinus massoniana* Lamb.) cell walls as related to microfibrillar angle," *Wood Fiber Sci.* 46(2), 228-236.
- Oliver, W. C., and Pharr, G. M. (1992). "An improved technique for determining hardness and elastic modulus using load and displacement sensing indentation experiments," *J. Mater Res.* 7(6), 1564-1583. DOI: 10.1557/JMR.1992.1564
- Olsson, A. M., Salmén, L., Eder, M., and Burgert, I. (2007). "Mechano-sorptive creep in wood fibres," *Wood Sci. Technol.* 41(1), 59-67. DOI: 10.1007/s00226-006-0086-5
- Salmén, L. (1982). "Temperature and water induced softening behaviour of wood fiber based materials," Ph.D. thesis, Kunigliga Tekniska Högskolan (KTH, Royal Institute of Technology), Stockholm, Sweden.
- Stelte, W., Clemons, C., Holm, J. K., Ahrenfeldt, J., Henriksen, U. B., and Sanadi, A. R. (2011). "Thermal transitions of the amorphous polymers in wheat straw," *Ind. Crops Prod.* 34(1), 1053-1056. DOI: 10.1016/j.indcrop.2011.03.014
- Struik, L. C. E. (1987). "The mechanical and physical ageing of semicrystalline polymers. 1.," *Polymer* 28(9), 1521-1533. DOI: 10.1016/0032-3861(87)90353-3
- Tze, W. T. Y., Wang, S., Rials, T. G., Pharr, G. M., and Kelley, S. S. (2007). "Nanoindentation of wood cell walls: Continuous stiffness and hardness measurements," *Composites, Part A.* 38(3), 945-953. DOI: 10.016/j.compositesa.2006.06.018
- Wagner, L., Bader, T. K., Auty, D., and de Borst, K. (2013). "Key parameters controlling stiffness variability within trees: a multiscale experimental-numerical approach," *Trees* 27(1), 321-336. DOI: 10.1007/s00468-012-0801-9
- Wagner, L., Bader, T. K., and de Borst, K. (2014). "Nanoindentation of wood cell walls: effects of sample preparation and indentation protocol," *J. Mater. Sci.* 49(1), 94-102. DOI: 10.1007/s10853-013-7680-3
- Yu, Y., Fei, B., Wang, H., and Tian, G. (2011). "Longitudinal mechanical properties of cell wall of Masson pine (*Pinus massoniana* Lamb.) as related to moisture content: A nanoindentation study," *Holzforschung* 65(1), 121-126. DOI: 10.1515./HF.2011.014

APPENDIX – RESULT DATABASE AND STATISTICAL ANALYSIS

The following Tables present the results of the nanoindentation tests in terms of mean and standard deviation of reduced modulus E_r , hardness H , and the two creep parameters $C1$ and $C2$, as well as the number of indents for all five investigated wood species in the S2 layer (Appendix Table 1) and the middle lamella (Appendix Table 2).

Appendix Table 1. Mean values, standard deviation (mean \pm sd) of reduced modulus (E_r), hardness (H), and the two creep parameters ($C1$ & $C2$) of the S2 layer of the five investigated wood species; n...number of indents.

RH	10%	40%	60%	80%	wet
	Pine				
E_r [GPa]	20.00 \pm 1.31	18.44 \pm 1.77*	17.33 \pm 1.43*	14.93 \pm 1.35*	2.96 \pm 1.14*
H [GPa]	0.48 \pm 0.02	0.43 \pm 0.02*	0.37 \pm 0.02*	0.26 \pm 0.02*	0.04 \pm 0.01*
$C1$ [%]	13.58 \pm 1.56	14.17 \pm 2.42	14.72 \pm 1.16	18.65 \pm 1.26*	27.13 \pm 6.01*
$C2$ [%]	10.16 \pm 1.38	9.97 \pm 0.73	10.43 \pm 0.75	13.42 \pm 0.81*	19.01 \pm 2.35*
n	21	17	14	19	10
	Spruce				
E_r [GPa]	22.16 \pm 1.55	20.35 \pm 1.15*	16.61 \pm 1.13*	14.86 \pm 1.05*	5.53 \pm 0.70*
H [GPa]	0.51 \pm 0.02	0.41 \pm 0.02*	0.30 \pm 0.02*	0.25 \pm 0.02*	0.07 \pm 0.01*
$C1$ [%]	14.32 \pm 1.95	14.26 \pm 1.40	17.38 \pm 1.41*	18.15 \pm 0.96*	21.35 \pm 2.53*
$C2$ [%]	9.02 \pm 0.86	10.06 \pm 0.52*	12.87 \pm 1.39*	13.13 \pm 1.04*	16.06 \pm 1.11*
n	15	21	20	17	12
	Yew				
E_r [GPa]	15.58 \pm 1.00	14.13 \pm 0.94*	13.66 \pm 1.77*	12.44 \pm 1.37*	4.41 \pm 1.07*
H [GPa]	0.48 \pm 0.03	0.43 \pm 0.02*	0.38 \pm 0.04*	0.32 \pm 0.05*	0.10 \pm 0.02*
$C1$ [%]	12.84 \pm 1.54	12.47 \pm 1.23	13.28 \pm 1.94	19.84 \pm 3.07*	22.31 \pm 4.44*
$C2$ [%]	10.21 \pm 1.82	9.51 \pm 0.73	9.54 \pm 1.55	13.83 \pm 1.66*	15.21 \pm 2.54*
n	19	20	18	7	11
	Oak				
E_r [GPa]	20.36 \pm 1.69	19.82 \pm 1.45	17.67 \pm 1.05*	15.70 \pm 1.40*	5.56 \pm 1.44*
H [GPa]	0.50 \pm 0.03	0.41 \pm 0.02*	0.33 \pm 0.02*	0.24 \pm 0.02*	0.07 \pm 0.01*
$C1$ [%]	13.83 \pm 0.94	14.41 \pm 0.93	15.92 \pm 1.42*	18.57 \pm 1.27*	23.53 \pm 2.89*
$C2$ [%]	10.37 \pm 1.29	10.59 \pm 1.10	11.93 \pm 0.95*	13.40 \pm 0.79*	15.35 \pm 1.15*
n	19	15	20	21	7
	Beech				
E_r [GPa]	19.92 \pm 1.35	19.35 \pm 0.96	18.32 \pm 1.14*	15.07 \pm 0.87*	4.29 \pm 1.09*
H [GPa]	0.50 \pm 0.04	0.41 \pm 0.02*	0.36 \pm 0.02*	0.27 \pm 0.02*	0.07 \pm 0.01*
$C1$ [%]	13.91 \pm 1.13	14.13 \pm 1.34	15.91 \pm 0.99*	20.50 \pm 1.80*	25.22 \pm 3.06*
$C2$ [%]	10.02 \pm 0.61	10.45 \pm 0.51	12.04 \pm 1.13*	14.39 \pm 1.07*	16.75 \pm 1.66*
n	18	26	22	18	7

*significantly different from 10% RH values ($p < 0.01$)

Appendix Table 2. Mean values, standard deviation (mean±sd) of reduced modulus (E_r), hardness (H), and the two creep parameters ($C1$ & $C2$) of the middle lamella of the five investigated wood species; n...number of indents.

RH	10%	40%	60%	80%	wet
Pine					
E_r [GPa]	8.50±0.80	7.24±0.33*	5.82±0.53*	4.49±0.43*	1.13±0.22*
H [GPa]	0.47±0.06	0.36±0.01*	0.29±0.01*	0.18±0.01*	0.05±0.01*
$C1$ [%]	14.94±2.24	13.63±0.51	14.48±0.56	19.87±1.38*	19.79±2.31*
$C2$ [%]	10.74±0.50	11.13±0.61	12.69±1.00*	15.27±0.73*	15.30±2.85*
n	14	15	14	16	5
Spruce					
E_r [GPa]	8.40±0.53	7.43±0.57*	5.94±0.90*	4.44±0.51*	1.62±0.51*
H [GPa]	0.42±0.01	0.35±0.01*	0.27±0.02*	0.18±0.02*	0.06±0.02*
$C1$ [%]	13.70±0.88	14.02±0.70	15.12±0.87*	20.86±1.08*	21.05±1.52*
$C2$ [%]	10.73±0.72	11.09±0.54	11.61±0.70*	14.85±0.51*	15.61±0.67*
n	9	17	18	8	5
Yew					
E_r [GPa]	7.84±0.33	7.48±0.31*	6.78±0.29*	6.07±0.67*	1.67±0.24*
H [GPa]	0.45±0.03	0.44±0.02	0.37±0.01*	0.30±0.04*	0.07±0.01*
$C1$ [%]	12.22±1.56	12.06±0.58	13.17±0.46	23.38±1.80*	22.25±2.33*
$C2$ [%]	9.46±0.75	9.28±0.39	10.37±0.42*	15.08±1.35*	15.12±2.90*
n	16	15	13	3	6
Oak					
E_r [GPa]	9.73±1.26	8.32±0.70*	7.05±0.46*	4.94±0.58*	2.66±0.52*
H [GPa]	0.40±0.04	0.32±0.02*	0.28±0.01*	0.15±0.01*	0.07±0.01*
$C1$ [%]	15.42±1.36	15.83±1.33	16.25±1.13	21.64±1.68*	21.69±3.81*
$C2$ [%]	12.20±1.06	12.27±0.79	12.59±0.66	15.84±1.76*	19.65±3.83*
n	16	13	10	12	5
Beech					
E_r [GPa]	8.76±0.51	8.04±0.45*	6.93±0.73*	5.04±0.40*	1.61±0.19*
H [GPa]	0.43±0.03	0.35±0.02*	0.30±0.03*	0.20±0.01*	0.05±0.01*
$C1$ [%]	14.09±1.09	14.38±0.79	15.99±1.15*	23.13±1.63*	18.88±3.13*
$C2$ [%]	11.02±0.77	11.64±0.79	12.41±0.67*	16.05±0.73*	15.50±1.18*
n	11	18	12	8	3

*significantly different from 10% RH values ($p < 0.01$)

Article submitted: February 24, 2015; Peer review completed: April 12, 2015; Revisions received and accepted: April 20, 2015; Published: May 15, 2015.

DOI: 10.15376/biores.10.3.4011-4025